COSMOS: A numerical relativity code specialized for PBH formation

Chul-Moon Yoo[1,2], **Albert Escrivà**[3], **Tomohiro Harada**[4], **Hayami Iizuka**[4], **Taishi Ikeda**[5], **Yasutaka Koga**[6], **Hirotada Okawa**[7], **Daiki Saito**[1], **Masaaki Shimada**[1], **and Koichiro Uehara**[1]

1 Graduate School of Science, Nagoya University, Japan **2** Kobayashi Maskawa Institute, Nagoya University, Japan **3** National Astronomical Observatory of Japan (NAOJ), Japan **4** Department of Physics, Rikkyo University, Japan **5** Center of Gravity, Niels Bohr Institute, Denmark **6** Yukawa Institute for Theoretical Physics, Kyoto University, Japan **7** Faculty of Software and Information Technology, Aomori University, Japan

DOI: 10.xxxxxx/draft

Software

- Review
- Repository
- Archive

Editor:

Submitted: 16 February 2025
Published: unpublished

Summary

Primordial black holes (PBHs) are black holes generated in the early universe without experience of the form of a star. It has been pointed out that PBHs may be candidates for black holes and compact objects of various masses in the universe or a major component of dark matter. In particular, PBHs have been attracting much attention in the recent development of gravitational wave observation. In the standard formation process, PBHs are formed from super-horizon primordial fluctuations with non-linearly large initial amplitude. In order to follow the whole non-linear gravitational dynamics, one has to rely on numerical relativity solving Einstein equations. `COSMOS` (Okawa et al., 2014; Yoo et al., 2013) and `COSMOS-S` (Yoo et al., 2022) provide simple tools for the simulation of PBH formation. `COSMOS` and `COSMOS-S` are C++ packages for solving Einstein equations in 3+1 dimensions and spherical symmetry (1+1 dimensions), respectively. It was originally translated from SACRA code (Yamamoto et al., 2008) into C++ and has been developed specialized for PBH formation. In this paper, we do not describe all scientific results obtained by using `COSMOS` or `COSMOS-S`. The readers who are interested in the past achievments may refer to Yoo et al. (2013); Okawa et al. (2014); Yoo & Okawa (2014); Okawa & Cardoso (2014); Ikeda et al. (2015); Brito et al. (2015); Brito et al. (2016); Okawa (2015); Yoo et al. (2017); Yoo et al. (2019); Yoo et al. (2022); Yoo (2024); Escrivà & Yoo (2024b); Escrivà & Yoo (2024a); Shimada et al. (2025) [1].

Statement of need

In the simulation of PBH formation, since there is a hierarchy between the size of the collapsing region and cosmological expansion scale, an efficient resolution refinement procedure is needed. In order to resolve the collapsing region, non-Cartesian scale-up coordinates (Yoo et al., 2019) and a fixed mesh-refinement procedure (Yoo, 2024) are implemented in `COSMOS`. The 1+1 dimensional simulation code `COSMOS-S` (Yoo et al., 2022) is derived from `COSMOS` with the CARTOON method (Alcubierre et al., 2001). To achieve a practically acceptable computational speed, an OpenMP package is used for the parallelization. No other packages are required, and the functionality is minimal. Therefore it would be easy to use for beginners of numerical

[1] In most of the references: Yoo et al. (2013); Okawa et al. (2014); Yoo & Okawa (2014); Okawa & Cardoso (2014); Ikeda et al. (2015); Brito et al. (2015); Brito et al. (2016); Okawa (2015); Yoo et al. (2017); Yoo et al. (2019); Yoo et al. (2022); Yoo (2024); Escrivà & Yoo (2024b); Escrivà & Yoo (2024a); Shimada et al. (2025), additional functions and packages have been implemented to meet the requirements for individual settings. Therefore the results may not be obtained by simply running the public code.

relativity. A perfect fluid with a linear equation of states and a massless scalar field are implemented as matter fields. Once users understand the source code to some extent, the system can be easily extended to various scientifically interesting settings.

Physical system settings

Einstein equations

$$G_{\mu\nu} = R_{\mu\nu} - \frac{1}{2}Rg_{\mu\nu} = \frac{8\pi G}{c^4}T_{\mu\nu}$$

are solved, where $G_{\mu\nu}$, $g_{\mu\nu}$, $R_{\mu\nu}$, R, G, c and $T_{\mu\nu}$ are the Einstein tensor, metric tensor, Ricci tensor, Ricci scalar, Newtonian gravitational constant, speed of light and energy momentum tensor, respectively. The energy momentum tensor is divided into the fluid and scalar field contributions as follows:

$$T_{\mu\nu} = T^{\rm SC}_{\mu\nu} + T^{\rm FL}_{\mu\nu}$$

with

$$T^{\rm SC}_{\mu\nu} = \nabla_\mu\phi\nabla_\nu\phi - \frac{1}{2}g_{\mu\nu}\nabla^\lambda\phi\nabla_\lambda\phi$$

and

$$T^{\rm FL}_{\mu\nu} = (\rho + P)u_\mu u_\nu + Pg_{\mu\nu},$$

where ∇, ϕ, ρ, u_μ and P are the covariant derivative associated with $g_{\mu\nu}$, scalar field, fluid energy density, four-velocity and pressure, respectively. The pressure and the energy density are assumed to satisfy the linear equation of state $P = w\rho$ with w being a constant. The equations of motion for the scalar field

$$\nabla^\mu\nabla_\mu\phi = 0$$

and the fluid

$$\nabla^\mu T^{\rm FL}_{\mu\nu} = 0$$

are also solved. Readers are asked to refer to standard textbooks of numerical relativity (e.g., Gourgoulhon (2012); Shibata (2016)) to learn how to rewrite these equations into a form suitable for numerical integration. To solve the fluid equations of motion, we basically follow the scheme discussed in Kurganov & Tadmor (2000); Shibata & Font (2005).

As for the initial data, we adopt the long-wavelength growing-mode solutions up through the next-leading order of the expansion parameter $\epsilon = k/(aH) \ll 1$, where $1/k$ gives the characteristic comoving scale of the inhomogeneity, and a and H are the scale factor and Hubble expansion rate in the reference background universe. The initial data can be characterized by a function of the spatial coordinates $\vec{x}$ as the curvature perturbation $\zeta(\vec{x})$ for adiabatic fluctuations (Harada et al., 2015; Yoo et al., 2020; Yoo, 2024) and iso-curvature perturbation $\Upsilon(\vec{x})$ for massless scalar iso-curvature (Yoo et al., 2022). Since the space is filled with the fluid, the initial fluid distribution can be generated to meet the constraint equations included in the Einstein equations. Then, the constraint equations are initially satisfied within the machine's precision. Therefore, the constraint equations are not solved by integrating elliptic differential equations. This is very different from the standard method to obtain the initial data for spacetimes with asymptotically flat vacuum regions. This is why elliptic solvers for constraint equations are not included in this package.

Examples

Several examples are included in the package. These examples are intended primarily for demonstration and instructional purposes, and thus, the precision is not a primary concern. The resolution has been intentionally kept to a minimum. In the figures below, the length scale is normalized by the size L of the box for the numerical simulation.

COSMOS (3+1 dimensional simulation)

- Evolution of a single-mode perturbation

The evolution of sinusoidal small fluctuation is given as an example, which can be compared with the corresponding linear perturbation (see Figure 1).

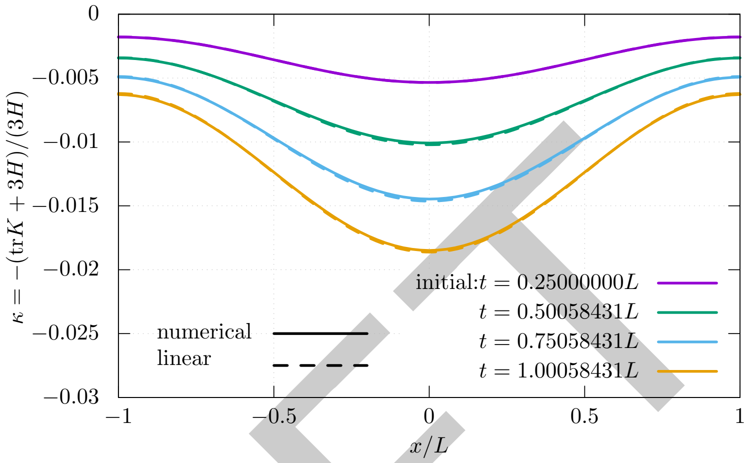

Figure 1: The time evolution of the trace of the extrinsic curvature tr$K$ is compared with the solution of the linear perturbation equation.

- Adiabatic spherically symmetric initial fluctuation

The scalar field is absent in this example. The setting is similar to that in Yoo et al. (2020). We also attach the data obtained by solving the Einstein equations until an apparent horizon is found (see Figure 2 and Figure 3).

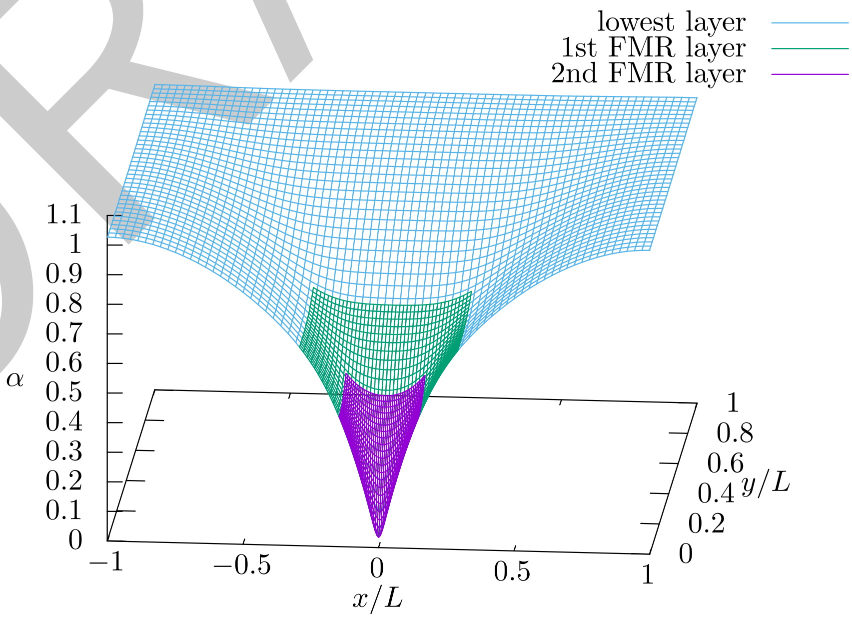

Figure 2: The lapse function ("tt-component" of the metric) on the xy-plane at the time when an apparent horizon is found.

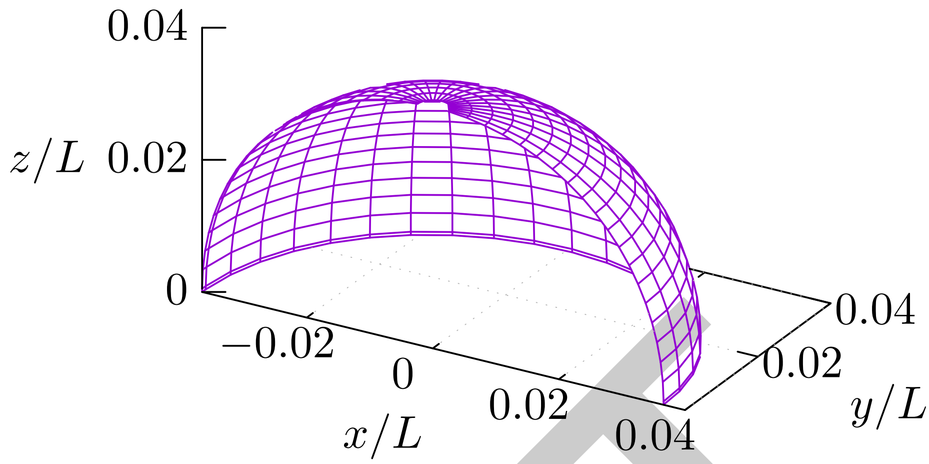

Figure 3: The shape of the apparent horizon when it is found.

- Spherically symmetric iso-curvature

The setting is similar to that in Yoo et al. (2022). We also attach the data obtained by solving the Einstein equations until an apparent horizon is found.

COSMOS-S (spherically symmetric simulation)

- Adiabatic spherically symmetric initial fluctuation

The physical parameter setting is the same as the corresponding example for the 3+1 dimensional simulation. However, the resolution is finer in this example of the spherically symmetric 1+1 code.

- Spherically symmetric iso-curvature

The physical parameter setting is the same as the corresponding example for the 3+1 dimensional simulation. However, the resolution is finer in this example of the spherically symmetric 1+1 code.

- Type II-B PBH formation

PBH formation from adiabatic fluctuation with extremely large initial amplitude is given as an example. The setting is similar to that in Uehara et al. (2025). One can find the non-trivial trapping horizon configuration as Figure 4.

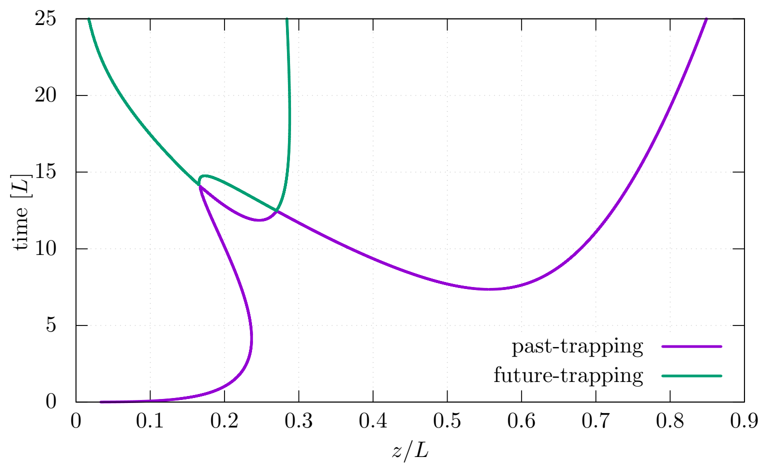

Figure 4: Trapping horizon trajectories.

Acknowledgements

A.E. acknowledges support from the JSPS Postdoctoral Fellowships for Research in Japan (Graduate School of Sciences, Nagoya University). K.U. would like to take this opportunity to thank the “THERS Make New Standards Program for the Next Generation Researchers” supported by JST SPRING, Grant Number JPMJSP2125. T.I. acknowledges support from VILLUM Foundation (grant no. VIL37766) and the DNRF Chair program (grant no. DNRF162) by the Danish National Research Foundation. This work is supported in part by JSPS KAKENHI Grant Nos. 20H05850 (C.Y.), 20H05853 (T.H., C.Y.), 21K20367 (Y.K.), 23KK0048 (Y.K.), 24K07027 (T.H., C.Y.) and 24KJ1223 (D.S.).

References

Alcubierre, M., Brandt, S., Bruegmann, B., Holz, D., Seidel, E., Takahashi, R., & Thornburg, J. (2001). Symmetry without symmetry: Numerical simulation of axisymmetric systems using Cartesian grids. *Int. J. Mod. Phys. D*, *10*, 273–290. https://doi.org/10.1142/S0218271801000834

Brito, R., Cardoso, V., Macedo, C. F. B., Okawa, H., & Palenzuela, C. (2016). Interaction between bosonic dark matter and stars. *Phys. Rev. D*, *93*(4), 044045. https://doi.org/10.1103/PhysRevD.93.044045

Brito, R., Cardoso, V., & Okawa, H. (2015). Accretion of dark matter by stars. *Phys. Rev. Lett.*, *115*(11), 111301. https://doi.org/10.1103/PhysRevLett.115.111301

Escrivà, A., & Yoo, C.-M. (2024a). *Non-spherical effects on the mass function of Primordial Black Holes*. https://arxiv.org/abs/2410.03451

Escrivà, A., & Yoo, C.-M. (2024b). *Simulations of Ellipsoidal Primordial Black Hole Formation*. https://arxiv.org/abs/2410.03452

Gourgoulhon, E. (2012). *3+1 formalism in general relativity : Bases of numerical relativity*. Springer. https://doi.org/10.1007/978-3-642-24525-1

Harada, T., Yoo, C.-M., Nakama, T., & Koga, Y. (2015). Cosmological long-wavelength solutions and primordial black hole formation. *Phys. Rev.*, *D91*(8), 084057. https://doi.org/10.1103/PhysRevD.91.084057

Ikeda, T., Yoo, C.-M., & Nambu, Y. (2015). Expanding universe with nonlinear gravitational waves. *Phys. Rev. D*, *92*(4), 044041. https://doi.org/10.1103/PhysRevD.92.044041

Kurganov, A., & Tadmor, E. (2000). New High-Resolution Central Schemes for Nonlinear Conservation Laws and Convection–Diffusion Equations. *J. Comput. Phys.*, *160*, 241–282. https://doi.org/10.1006/jcph.2000.6459

Okawa, H. (2015). Nonlinear evolutions of bosonic clouds around black holes. *Classical and Quantum Gravity*, *32*(21), 214003. https://doi.org/10.1088/0264-9381/32/21/214003

Okawa, H., & Cardoso, V. (2014). Black holes and fundamental fields: Hair, kicks, and a gravitational Magnus effect. *Phys. Rev. D*, *90*(10), 104040. https://doi.org/10.1103/PhysRevD.90.104040

Okawa, H., Witek, H., & Cardoso, V. (2014). Black holes and fundamental fields in Numerical Relativity: initial data construction and evolution of bound states. *Phys. Rev. D*, *89*(10), 104032. https://doi.org/10.1103/PhysRevD.89.104032

Shibata, M. (2016). *Numerical relativity*. World Scientific Publishing Co. Pte. Ltd. https://doi.org/10.1142/9692

Shibata, M., & Font, J. A. (2005). Robustness of a high-resolution central scheme for hydrodynamic simulations in full general relativity. *Phys. Rev. D*, *72*, 047501. https://doi.org/10.1103/PhysRevD.72.047501

Shimada, M., Escrivá, A., Saito, D., Uehara, K., & Yoo, C.-M. (2025). Primordial black hole formation from type II fluctuations with primordial non-Gaussianity. *JCAP*, *02*, 018. https://doi.org/10.1088/1475-7516/2025/02/018

Uehara, K., Escrivà, A., Harada, T., Saito, D., & Yoo, C.-M. (2025). Numerical simulation of type II primordial black hole formation. *JCAP*, *01*, 003. https://doi.org/10.1088/1475-7516/2025/01/003

Yamamoto, T., Shibata, M., & Taniguchi, K. (2008). Simulating coalescing compact binaries by a new code SACRA. *Phys. Rev. D*, *78*, 064054. https://doi.org/10.1103/PhysRevD.78.064054

Yoo, C.-M. (2024). Primordial black hole formation from a nonspherical density profile with a misaligned deformation tensor. *Phys. Rev. D*, *110*(4), 043526. https://doi.org/10.1103/PhysRevD.110.043526

Yoo, C.-M., Harada, T., Hirano, S., Okawa, H., & Sasaki, M. (2022). Primordial black hole formation from massless scalar isocurvature. *Phys. Rev. D*, *105*(10), 103538. https://doi.org/10.1103/PhysRevD.105.103538

Yoo, C.-M., Harada, T., & Okawa, H. (2017). 3D Simulation of Spindle Gravitational Collapse of a Collisionless Particle System. *Class. Quant. Grav.*, *34*(10), 105010. https://doi.org/10.1088/1361-6382/aa6ad5

Yoo, C.-M., Harada, T., & Okawa, H. (2020). Threshold of Primordial Black Hole Formation in Nonspherical Collapse. *Phys. Rev. D*, *102*(4), 043526. https://doi.org/10.1103/PhysRevD.102.043526

Yoo, C.-M., Ikeda, T., & Okawa, H. (2019). Gravitational Collapse of a Massless Scalar Field in a Periodic Box. *Class. Quant. Grav.*, *36*(7), 075004. https://doi.org/10.1088/1361-6382/ab06e2

Yoo, C.-M., & Okawa, H. (2014). Black hole universe with a cosmological constant. *Phys. Rev. D*, *89*(12), 123502. https://doi.org/10.1103/PhysRevD.89.123502

Yoo, C.-M., Okawa, H., & Nakao, K. (2013). Black Hole Universe: Time Evolution. *Phys. Rev. Lett.*, *111*, 161102. https://doi.org/10.1103/PhysRevLett.111.161102